DELFT UNIVERSITY OF TECHNOLOGY

REPORT 06-04

A STUDY OF ENTHALPY METHODS FOR MARK FORMATION
MODELING

J.H. BRUSCHE, A. SEGAL, C. VUIK

A study of enthalpy methods for mark formation modeling

J.H. Brusche, A. Segal., C. Vuik[1]

March 24, 2006

[1]Delft University of Technology, Faculty of Electrical Engineering, Mathematics and Computer Science, Department of Applied Mathematical Analysis, P.O. Box 5031, 2600 GA Delft, The Netherlands, phone: 31 15 2787608, fax: 31 15 2787209 ([j.h.brusche, a.segal, c.vuik]@tudelft.nl)

Contents

Chapter 1

Introduction

The modeling of the writing of an amorphous mark in the crystalline background of the phase-change layer of a rewritable optical disk, such as the Blu-ray disk, presents an interesting numerical challenge. As a result of a short, locally intense, heating up by a focused laser beam, the illuminated region of the crystalline material melts. After the laser pulse, due to rapidly cooling down, the molten region solidifies, resulting in a solid amorphous mark.

A specific moving boundary problem, a so called Stefan problem, can be formulated to describe the growth process of the mark. In this formulation, the outer boundary of the expanding molten region acts as an additional unknown. Various numerical approaches can be applied in order to solve this Stefan problem. In the present document the possibilities of techniques, based on the enthalpy method, are explored. In the enthalpy formulation, the Stefan condition that describes the position of the moving front, is implicitly incorporated. In this way, explicitly dealing with the inherent difficulties that are related to the discontinuities of the temperature across the moving boundary is avoided.

In this study the two phase Stefan problem that describes the mark formation is considered for two cases: one in which the physical parameters are assumed to be equal in both phases (this is of course non-physical, but mathematically interesting) and the other case in which the parameters differ in both phases.

In the Chapter 2 some theory and results of various numerical techniques with respect to the enthalpy method will be presented. These techniques include the Kirchoff transformation, a non-linear successive over-relaxation (SOR) method, application of a superficial phase-change linear, relaxed linearization and a pseudo-Newton iterative method.

In the concluding chapter an overview of the results is given.

Chapter 2

Fully implicit enthalpy

The goal of this study is to solve the enthalpy formulation of the two-phase Stefan problem as discussed in the literature study [3]. A variety of numerical methods as described in [3] have been implemented and tested for a 1D finite volumes formulation. In most experiments, the temperature T was replaced by the Kirchoff temperature u.

2.1 Problem description

The two-phase Stefan problem on a three-dimensional domain Ω with fixed outer boundary $\delta\Omega$ and moving boundary $\Gamma(t)$ is given by [3]:

$$
\begin{cases}
\rho c \dfrac{\partial T(\boldsymbol{x}, t)}{\partial t} = \nabla \cdot (\kappa \nabla T(\boldsymbol{x}, t)) + Q(\boldsymbol{x}, t) & \forall \boldsymbol{x} \in \Omega_{1,2}, t > 0 \qquad \text{(2.1a)} \\[2ex]
+\rho L v_n = \left[\kappa \dfrac{\partial T}{\partial n} \right], \quad T = T_m & \text{for } \boldsymbol{x} = \Gamma(t), t > 0 \qquad \text{(2.1b)} \\[2ex]
T(\boldsymbol{x}, 0) = \bar{T}_1(\boldsymbol{x}) & \forall \boldsymbol{x} \in \Omega_{1,2}, t > 0 \qquad \text{(2.1c)}
\end{cases}
$$

where we have set $t_0 = 0$, together with one or more of the following boundary conditions on the complementary parts $\delta\Omega_i, i = 1, 2, 3$ of the fixed outer boundary $\delta\Omega = \bigcup_{i=1}^{3} \delta\Omega_i$:

1. A Dirichlet condition on $\delta\Omega_1$:

$$
T = \bar{T}_2(\boldsymbol{x}). \tag{2.2}
$$

2. A Neumann condition on $\delta\Omega_2$:

$$
\kappa(T) \frac{\partial T}{\partial \boldsymbol{n}}(\boldsymbol{x}) = \bar{q}(\boldsymbol{x}), \tag{2.3}
$$

where $\mathbf{n}$ is the outward unit normal to the boundary surface, and $\bar{q}(\boldsymbol{x})$ a given normal heat flux.

3. A radiation-type boundary condition on $\delta\Omega_3$:

$$\kappa(T)\frac{\partial T}{\partial \boldsymbol{n}}(\boldsymbol{x}) = \bar{\alpha}(T), \tag{2.4}$$

where $\bar{\alpha}(T)$ is a non-linear function of temperature.

In the enthalpy formulation the heat conduction equation and the Stefan condition are replaced by what is known as the enthalpy equation (in differential form):

$$H_t + \operatorname{div} \mathbf{q} = Q, \tag{2.5}$$

where H is the enthalpy function. In this study we will mostly restrict ourselves to isothermal phase-change (that is, a melting point $T = T_m$, instead of a melting trajectory). Besides, we will consider only problems in which the physical parameters $\rho, c_s, c_l, \kappa_s, \kappa_l$ are constants. Subject to these assumptions, the enthalpy function is given by:

$$H = \begin{cases} \rho c_s(T - T_m), & T \leq T_m \\ \rho c_l(T - T_m) + \rho L, & T > T_m \end{cases} \tag{2.6}$$

2.2 Employing the Kirchoff transform

According to [1], p. 216, the Kirchoff temperature is "the best choice for the enthalpy scheme since it is consistent with the mushy nodes being treated as isothermal." Besides, "faster convergence is observed in the iterative scheme, making it more efficient", [1], p. 224. Alexiades et al. present the enthalpy formulation, which could be referred to as "Voller's enthalpy formulation", in [1], Chapter 4.3.E. Because of the inherent advantages of applying the Kirchoff transform, we next present the enthalpy formulation and consecutively the Elliott-Ockendon SOR scheme, in case the Kirchoff transformation is applied.

The normalized Kirchoff transformed temperature for constant κ_s, κ_l is given by

$$u = \begin{cases} \kappa_s(T - T_m) & T < T_m \\ 0 & T = T_m \\ \kappa_l(T - T_m) & T > T_m \end{cases}. \tag{2.7}$$

The corresponding enthalpy is

$$H = \begin{cases} \frac{\rho c_s u}{\kappa_s} & u \leq 0 \\ \frac{\rho c_l u}{\kappa_l} + \rho L & u > 0 \end{cases}. \tag{2.8}$$

The 1D finite volumes discretization of equation (2.5), using central differences in space and Euler backward in time, yields:

$$\frac{H_i^{n+1} - H_i^n}{\Delta t_n} - \frac{u_{i-1}^{n+1} - 2u_i^{n+1} + u_{i+1}^{n+1}}{\Delta x^2} = Q_i^{n+1}, \tag{2.9}$$

which after rearranging terms results in:

$$H_i^{n+1} + 2\frac{\Delta t}{\Delta x^2} u_i^{n+1} = \Delta t Q_i^{n+1} + H_i^n + \frac{\Delta t}{\Delta x^2}(u_{j-1}^{(p+1)} + u_{j+1}^{(p)}). \tag{2.10}$$

By giving names to the known terms, as in [1]:

$$C_j = 2\frac{\Delta t}{\Delta x^2}, \tag{2.11}$$

$$b_j^n = \Delta t Q_i^{n+1} + H_i^n, \tag{2.12}$$

$$z_j^{(p)} = b_j^n + \frac{\Delta t}{\Delta x^2}(u_{j-1}^{(p+1)} + u_{j+1}^{(p)}), \tag{2.13}$$

$$\tag{2.14}$$

where the superscript (p) denotes the iteration number, and n the previous time level, we have the following system of equations (Gauss-Seidel):

$$H_j^{(p+1)} + C_j u_j^{(p+1)} = z_j^{(p)}. \tag{2.15}$$

Consequently, the iteration process transforms into:

1. Compute C_j and $z_j^{(p)}$.

2. Compute $\tilde{u}_j^{(p+1)}$ from

$$\tilde{u}_j^{(p+1)} = \begin{cases} \frac{z_j^{(p)}}{\rho c_s/\kappa_s + C_j} & z_j^{(p)} \leq 0, \\ 0 & 0 < z_j^{(p)} < \rho L, \\ \frac{z_j^{(p)} - \rho L}{\rho c_l/\kappa_l + C_j} & z_j^{(p)} \geq \rho L \end{cases}. \tag{2.16}$$

3. Set $\hat{u}_j^{(p+1)} = u_j^{(p)} + \omega[\tilde{u}_j^{(p+1)} - u_j^{(p)}]$ (Over-relaxation).

4. Set

$$u_j^{(p+1)} = \begin{cases} \hat{u}_j^{(p+1)} & \text{if } \hat{u}_j^{(p+1)} \cdot u_j^{(p)} > 0, \\ \tilde{u}_j^{(p+1)} & \text{if } \tilde{u}_j^{(p+1)} \cdot u_j^{(p)} \leq 0 \end{cases}, \qquad (2.17)$$

that is, only over-relax the nodes that have not just changed phase.

5. If a convergence criterion, say $\|u_j^{(p+1)} - u_j^{(p)}\| < tolerance$, is satisfied, then set $u_j^{n+1} = u_j^{(p+1)}$, hence

$$T_j^{n+1} = \begin{cases} T_m + u_j^{n+1}/\kappa_s & u_j^{n+1} < 0, \\ T_m & u_j^{n+1} = 0, , \\ T_m + u_j^{n+1}/\kappa_l & u_j^{n+1} > 0, \end{cases} \qquad (2.18)$$

and $H_j^{n+1} = z_j^{(p)} - C_j \cdot u_j^{n+1}$.

2.3 Equal parameters

We have implemented the implicit scheme as described above in Matlab for the case, where the diffusivities κ_s, κ_l and the heat capacities c_s, c_l are taken to be constants. The Matlab code has been first tested on a numerical example taken from [4] in which the properties for both the liquid and the solid are the same. The thermal properties for the example are: $\rho = 1 kg/m^3, \kappa = 2W/m°C, c = 2.5 \times 10^6 J/kg°C$, and $L = 1 \times 10^8 J/kg$. The initial temperature on the whole domain is $2°C$, the melting temperature $T_m = 0°C$. On the left end, a Dirichlet boundary condition is imposed, $T = -4°C$, and on the right end we have the insulation condition, $\partial T/\partial t = 0$. We use a mesh consisting of 100 grid points; the grid spacing being $\Delta x = 0.1m$ and the time step $\Delta t = 21600s$.

In Figure 2.1 the temperature in a point $x = 0.3m$ from the left boundary has been plotted as a function of the time in days. Both the analytical and the numerical solution are shown. Note that the numerical solution has a 'staircase' shape. In [1], p. 219-220 an explanation is provided: "The 'staircase' shape is characteristic of enthalpy methods and it is much more pronounced for a lesser number of grid points. This is due to the fact that while the interface lies anywhere inside a particular mesh interval, the temperature of that interval is held at T_m, so the temperature in the rest of the slab relaxes to a steady state corresponding to a fixed isotherm through that node. When the interface moves to the next mesh interval, the temperature adjusts rapidly and then relaxes to a new steady state. It follows that the duration of each 'step' is strictly a function of the time the interface remains in each interval, and therefore, the finer the mesh the shorter the 'steps'."
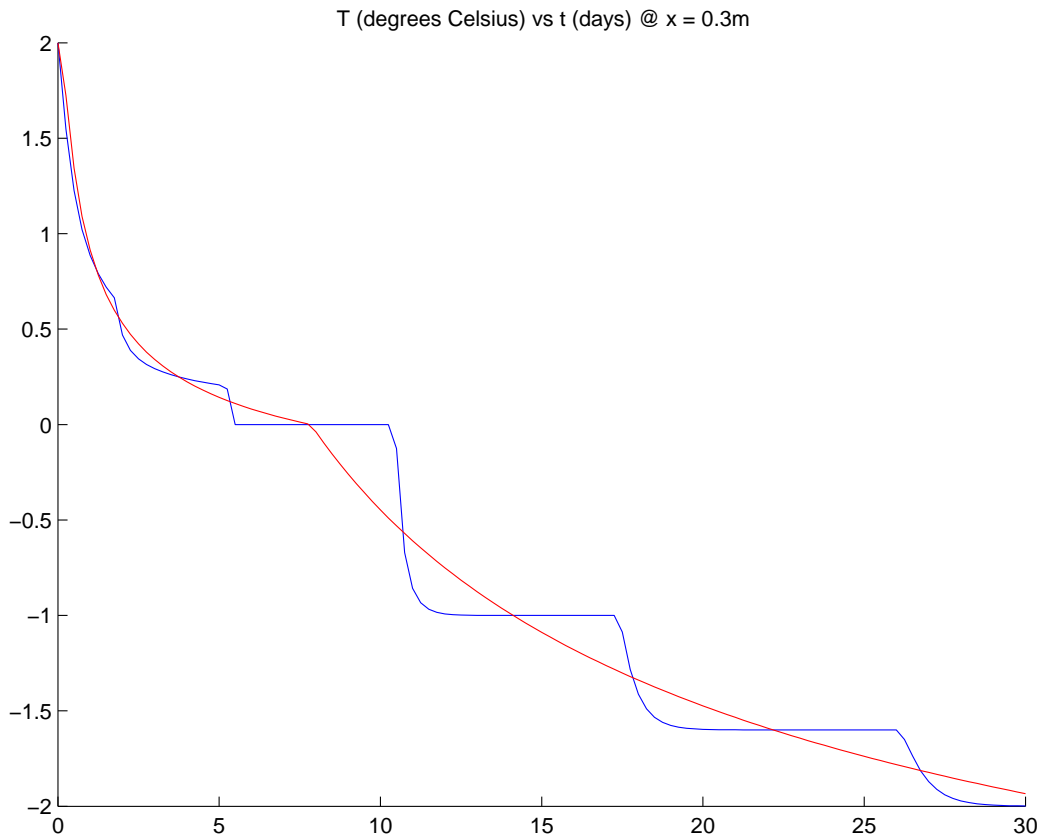
Figure 2.1: Numerical and analytical solution in case of equal thermal properties for the grid point at $x = 0.3m$.

2.4   Unequal parameters

When the thermal properties of the liquid and solid phase are not the same, the example becomes much more interesting. In particular since the Kirchoff transformation now takes effect. Once again we used the parameters as given in [4], which are: $\kappa_s = 2.22W/m°C, \kappa_l = 0.556W/m°C, c_s = 1.762 \times 10^6 J/kg°C, c_l = 4.226 \times 10^6 J/kg°C, L = 3.38 \times 10^8 J/kg$, and $\rho = \rho_s = \rho_l = 1kg/m^3$. On the whole domain the initial temperature is now $10°C$, while the melting temperature is again set to be $T_m = 0°C$. The temperature at the left boundary is kept at $-20°C$, the right end is again insulated. The grid spacing and the time step are $\Delta x = 0.1m$ and $\Delta t = 2000s$. The temperature as function of the time is shown in Figure 2.2 for a grid point $x = 0.3m$ from the left boundary. Note that as could be expected, the 'staircase' effect also occurs in case the thermal properties of the phases are unequal.
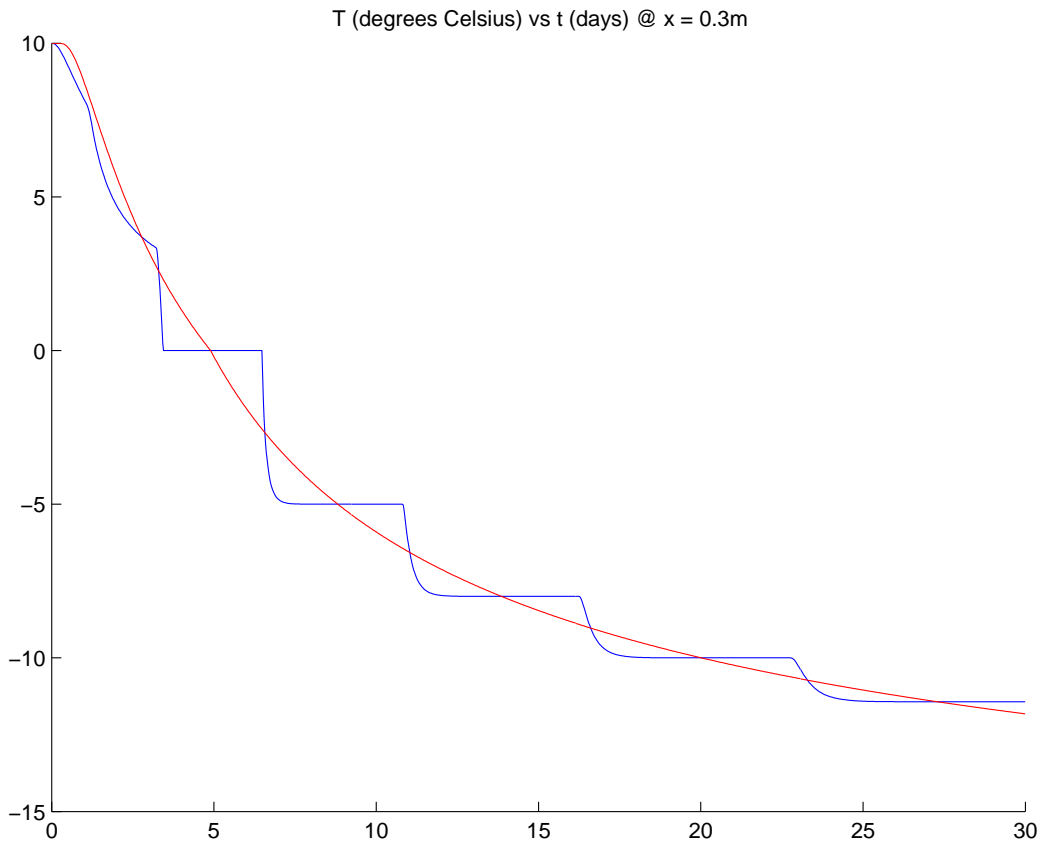
Figure 2.2: Numerical and analytical solution in case of unequal thermal properties for the grid point at $x = 0.3m$.

2.5   Sepran implementation

The Sepran implementation of "Voller's method" in combination with Elliott-Ockendon SOR requires some adjustments to be made with concern to the solution algorithm. Next we present a short overview of the finite element equivalent to the previously described finite volume formulation.

Starting point is the enthalpy equation:

$$\frac{\partial H}{\partial t} - \nabla(\kappa \nabla T) = Q, \tag{2.19}$$

subject to the boundary conditions on the disjunct boundaries $\partial\Omega_1, \partial\Omega_2$, $\partial\Omega_1 \cup \partial\Omega_2 = \partial\Omega$:

$$T = T_1, \qquad \text{for } x \in \partial\Omega_1, \tag{2.20}$$

$$\frac{\partial T}{\partial x} = 0, \qquad \text{for } x \in \partial\Omega_2. \tag{2.21}$$

Using the standard basis functions ϕ and the standard Galerkin approximations

$$T(t) = \sum_{j=1}^{N+N_b} T_j(t)\phi_j, \qquad H(t) = \sum_{j=1}^{N+N_b} H_j(t)\phi_j, \qquad (2.22)$$

where N denotes the number of nodal points $\notin \partial\Omega_1$, the system of Galerkin equations is given by:

$$\sum_{j=1}^{N+N_b} \left\{ \frac{\partial H_j}{\partial t} \int_\Omega \phi_j\phi_i d\Omega + T_j \int_\Omega \kappa \nabla\phi_j \nabla\phi_i d\Omega \right\} = \int_\Omega Q_i\phi_i d\Omega, \qquad (2.23)$$

for $i = 1, 2, \ldots, N$. Or in matrix-vector notation:

$$M\frac{\partial \mathbf{H}}{\partial t} + S\mathbf{T} = \mathbf{b}. \qquad (2.24)$$

In case Euler backward is applied for the time integration, the final system is given by:

$$M\frac{\mathbf{H}^{n+1} - \mathbf{H}^n}{\Delta t} + S\mathbf{T}^{n+1} = \mathbf{b}^{n+1}. \qquad (2.25)$$

If we let $\tilde{M}$ be the lumped version of the mass matrix M and D the diagonal of the stiffness matrix S, then for a Kirchoff transformed temperature u the third step of the iteration process as described in Section 2.2 is replaced by: Compute $\tilde{u}_j^{(p+1)}$ from

$$\tilde{u}_j^{(p+1)} = \begin{cases} \dfrac{z_j^{(p)}}{D_{jj}\Delta t + \tilde{M}_{jj}\rho c_s/\kappa_s} & z_j^{(p)} \leq 0, \\ 0 & 0 < z_j^{(p)} < \tilde{M}_{jj}\rho L, \\ \dfrac{z_j^{(p)} - \tilde{M}_{jj}\rho L}{D_{jj}\Delta t + \tilde{M}_{jj}\rho c_l/\kappa_l} & z_j^{(p)} \geq \tilde{M}_{jj}\rho L \end{cases} . \qquad (2.26)$$

The enthalpy is updated according to:

$$H_j^{n+1} = (z_j^{(p)} - D_{jj}\Delta t \cdot u_j^{n+1})/\tilde{M}_{jj} \qquad (2.27)$$

In order to study the influence of the number of grid points on the 'staircasing' effect, we have computed the numerical solution of the test problem as described in Section 2.3 in case the number of grid points $N = 99$, $N = 999$ and $N = 9999$. As can be concluded from Figure 2.3, for $N = 999$ the 'staircasing' is far less than for $N = 99$. However, when the number of grid points is increased up to $N = 9999$ some unexpected oscillations appear before the actual melting of the point at $x = 0.3m$. Most probably, these oscillations can be described as an effect of the tolerance parameter for the convergence test being too large in comparison to the fineness of the mesh.
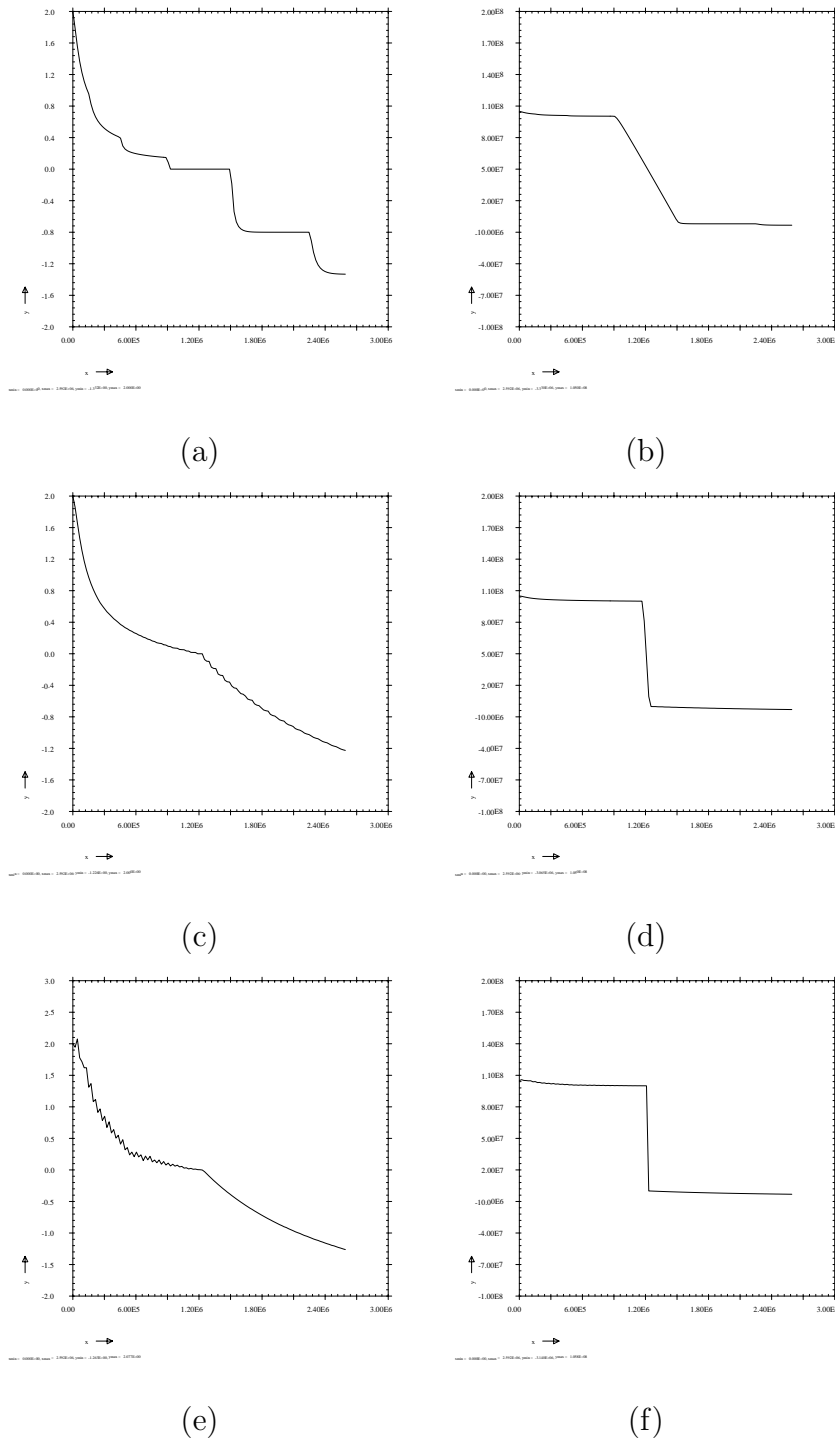
(a)

(b)

(c)

(d)

(e)

(f)

Figure 2.3: The influence of the number of grid-points N for the test example of Section 2.3. (a), (b) $N = 99$; (c), (d) $N = 999$; (e), (f) $N = 9999$. The figures to the left show the temperature history for a point for which $x = 0.3m$, the right figures the corresponding enthalpies.

2.6   A superficial phase-change range

In an attempt to remove or at least lessen the "staircase" like behavior as seen in the temperature profiles for the "Voller" approach, we have implemented a finite volume version of the "superficial phase-change range technique" as proposed by Bhattacharya et al. [2].

Instead of an isothermal jump at the melting temperature T_m, Bhattacharya et al. assume a melting trajectory, during which the temperature changes linearly between an initial temperature $T_I < T_m$ and a final temperature $T_F > T_m$. The total width of the superficial phase-change range around T_m is denoted as ΔT. In order to implement this approach in the enthalpy method, the functional ϕ_l, called the liquid volume fraction, is defined as

$$\phi_l = \begin{cases} 0 & T \leq T_I, \\ \frac{T-T_I}{T_F-T_I} & T_I \leq T \leq T_F, \\ 1 & T \geq T_F, \end{cases} \tag{2.28}$$

with $T_I = T_m - \Delta T/2$ and $T_F = T_m + \Delta T/2$.

Using ϕ_l, the (source free) enthalpy equation is rewritten as

$$\frac{\partial H}{\partial t} - \nabla(\kappa_{eff}\nabla T) = 0, \tag{2.29}$$

where $\kappa_{eff} = \phi_l\kappa_l + (1 - \phi_l)\kappa_s$ is the effective thermal conductivity.

The total enthalpy is written in functional form as:

$$H(T) = \rho(1 - \phi_l)\int_{T_R}^{T} c_s d\alpha + \rho\phi_l \left[\int_{T_R}^{T_I} c_s d\alpha + L + \int_{T_I}^{T} c_l d\alpha\right], \tag{2.30}$$

where T_R represents an arbitrary reference temperature.

For a simplified case, in which the physical parameters are considered to be constant and equal in both phases, we have implemented the above described formulation in Matlab, in combination with the Elliott-Ockendon SOR iterative resolution scheme. We remark that in the actual Matlab code unequal conductivities are allowed for.

Under the given assumptions, the effective conductivity $\kappa_{eff} = \kappa_s = \kappa_l = \kappa$. If we introduce the normalized temperature $u = T_m - T_I$ and choose the reference temperature T_R to be T_I, the functional form of $H(T)$ simplifies to

$$H(T) = \rho(1 - \phi_l)c_s u + \rho\phi_l\left[L + c_l u\right]. \tag{2.31}$$

As a result, the third step of the Elliott-Ockendon SOR scheme now becomes:

Compute $\tilde{u}_j^{(p+1)}$ from

$$\tilde{u}_j^{(p+1)} = \begin{cases} \dfrac{z_j^{(p)}}{C_j^{(p)}+\rho c_s} & z_j^{(p)} \leq 0, \\[2ex] \dfrac{z_j^{(p)}}{C_j^{(p)}+\rho c_s+\rho L/(T_F-T_I)} & 0 < z_j^{(p)} < \rho L + (\rho c_l + C_j^{(p)})(T_F - T_I), \\[2ex] \dfrac{z_j^{(p)}-\rho L}{C_j^{(p)}+\rho c_l} & z_j^{(p)} \geq \rho L + (\rho c_l + C_j^{(p)})(T_F - T_I), \end{cases} \tag{2.32}$$

where $C_j^{(p)}$ and $z_j^{(p)}$ are now given by

$$C_j^{(p)} = 2\kappa \frac{\Delta t}{\Delta x^2}, \tag{2.33}$$

$$z_j^{(p)} = b_j^n + \kappa \frac{\Delta t}{\Delta x^2}(u_{j-1}^{(p+1)} + u_{j+1}^{(p)}). \tag{2.34}$$

$$\tag{2.35}$$

Note that in case of constant physical parameters, that might be unequal in both phases, for $0 \leq u \leq T_F - T_I$ the following relation between $\tilde{u}_j^{(p)}$ and $z_j^{(p)}$ can be derived (for the sake of clarity we leave out non-relevant superscripts and subscripts):

$$\left(\frac{\rho c_l}{T_F - T_I} - \frac{\rho c_s}{T_F - T_I}\right)\tilde{u}^2 + \left(C + \rho c_s + \frac{\rho L}{T_F - T_I}\right)\tilde{u} = z. \tag{2.36}$$

For $c_s = c_l$, the quadratic term cancels and the expression for $\tilde{u}$ as it appears in (2.32) can be easily obtained. For $c_s \neq c_l$ the positive root should be taken in order to obtain convergence to the correct solution.

Some results are shown in Figures 2.4 and 2.5. From Figure 2.4 it can be concluded that the choice of ΔT does not lessen the 'staircase' behavior in time of the numerical solution for the temperature. What changes is the slope of the graph around the melting point.

The speed at which the melting process progresses, which can be expressed by the Stefan number, defined as:

$$St = \frac{\rho c_l(T_{ref} - T_m)}{L}, \tag{2.37}$$

affects the performance of the 'Bhattacharya' method, as becomes clear from Figure 2.5. As can be concluded from Figure 2.5 (a) - (c) the higher the Stefan number is, the lesser the 'stair-casing' effect. Apparently, the 'Bhattacharya' approach shows a lesser degree of 'stair-casing' than the standard 'Voller' scheme, as shown in Figures 2.5 (d) - (f).
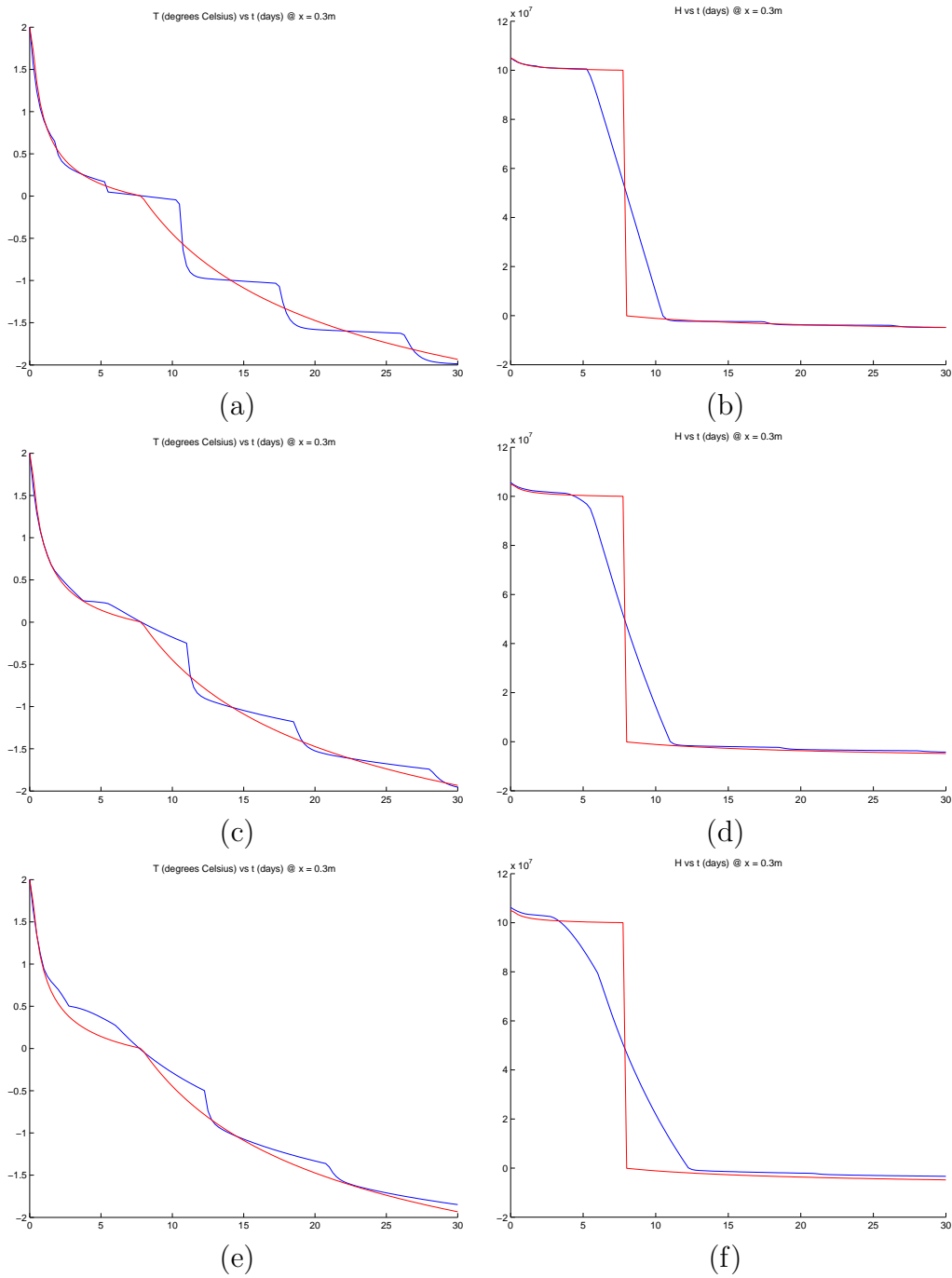
Figure 2.4: The influence of the choice of ΔT for the test example of Section 2.3. (a), (b) $\Delta T = 0.1$; (c), (d) $\Delta T = 0.5$; (e), (f) $\Delta T = 1$. All figures show both the numerical (blue) as well as the analytical (red) solution. The figures to the left show the temperature history for a point for which $x = 0.3m$, the right figures the corresponding enthalpies.
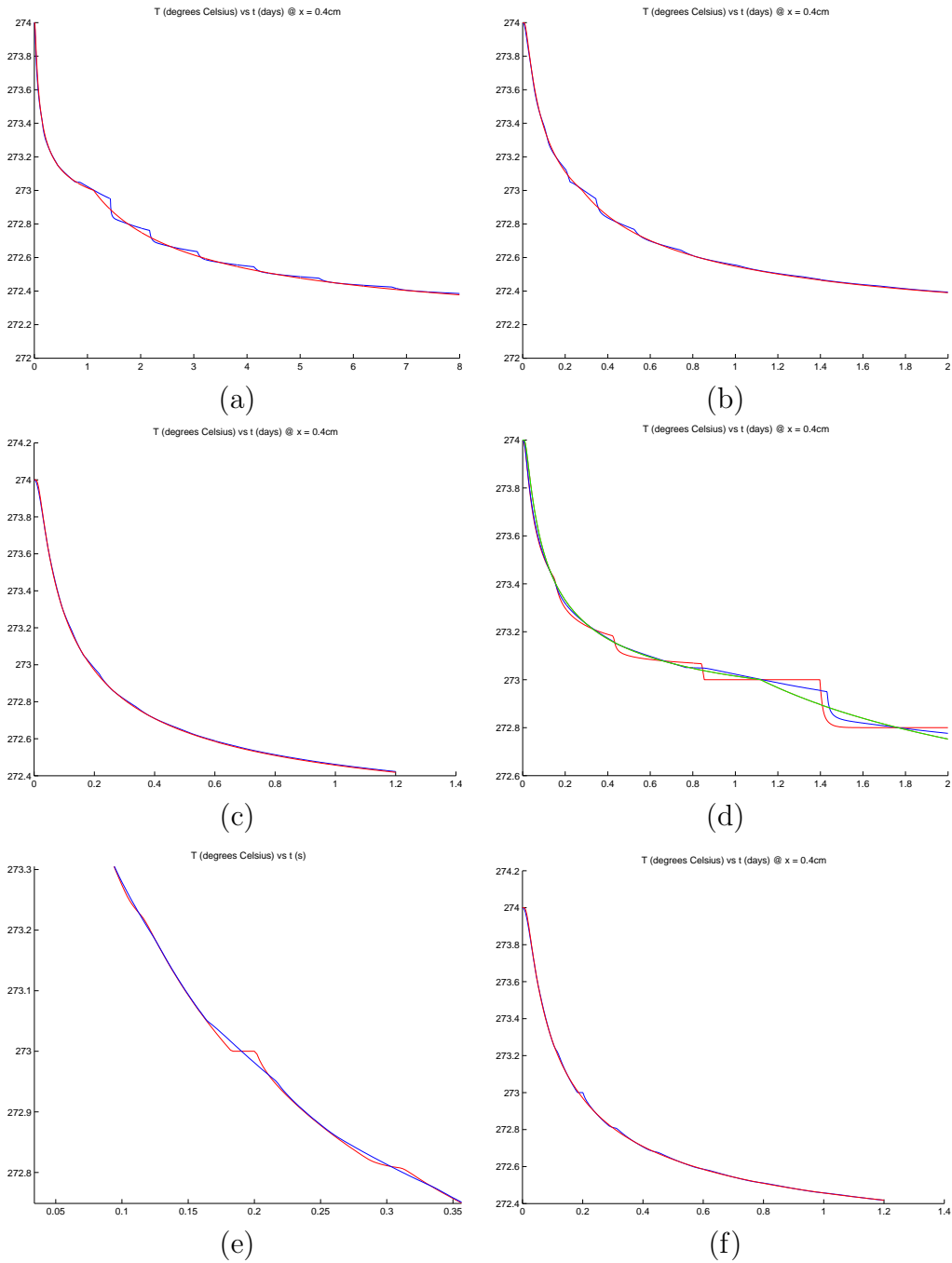
Figure 2.5: The temperature history of a point at $x = 0.4cm$ for the melting problem by Bhattacharya as mentioned in Section 2.6, with $\Delta T = 0.1$. (a), (b), (c) Numerical results compared to the analytical solution for Stefan numbers $St = 0.1, St = 1$ and $St = 10$ respectively. (d) Comparison of the analytical (green), 'Voller' (red) and 'Bhattacharya' (blue) solution for $St = 0.1$. (e) Comparison of the 'Voller' (red) and 'Bhattacharya' (blue) solution for $St = 10$ (fragment). (f) The 'Voller' solution compared to the analytical solution for $St = 10$ (compare with (c)).

2.7   Relaxed linearization and pseudo-Newton iteration

Another approach that we have considered is the one described by Nedjar [5]. Starting point of our derivation is the following discretized enthalpy equation in matrix-vector form:

$$R(\mathbf{u}) \equiv \frac{\mathbf{H}_{n+1} - \mathbf{H}_n}{\Delta t} - A\mathbf{u}_{n+1} - \mathbf{b}_{n+1} = \mathbf{0}, \tag{2.38}$$

where $\mathbf{u}$ denotes the Kirchoff transformed temperature, A is the standard central discretization matrix for the second derivative and $\mathbf{b}$ contains information on the boundary conditions and/or a source. Note that we have chosen the Euler backward scheme for the time discretization.

Typically, due to the non-linear nature of the enthalpy function $\mathbf{H}(\mathbf{u})$, one could consider a linearization $DR(\mathbf{u})$ of $R(\mathbf{u})$ and, accordingly, solve a sequence of successive linearized problems

$$DR(\mathbf{u}^{(p)})\Delta\mathbf{u}^{(p)} = -R(\mathbf{u}^{(p)}), \tag{2.39}$$

where $\Delta\mathbf{u}^{(p)} = \mathbf{u}^{(p+1)} - \mathbf{u}^{(p)}$ is the temperature increment in iteration p, until the residual $R(\mathbf{u}^{(p)})$ vanishes to within a pre-described tolerance. Next we will discuss a relaxed version of this approach, which could be best described as a pseudo-Newton iterative scheme.

The main idea of the proposed algorithm by Nedjar is to consider a relaxed linearization of the temperature versus enthalpy relation, $\mathbf{u} = \tau(\mathbf{H})$, instead of the classical enthalpy-temperature relation. The linearization of the function $\tau(\mathbf{H})$, neglecting any higher order terms, is given by

$$\mathbf{u}^{(p+1)} \equiv \mathbf{u}^{(p)} + \Delta\mathbf{u}^{(p)} \simeq \tau(\mathbf{H}^{(p)}) + \tau'(\mathbf{H}^{(p)})\Delta\mathbf{H}^{(p)}, \tag{2.40}$$

where $\Delta\mathbf{H}^{(p)} = \mathbf{H}^{(p+1)} - \mathbf{H}^{(p)}$, and $\tau'(\mathbf{H}^{(p)})$ is the derivative of τ with respect to its argument. Equation (2.40) can be rewritten as

$$\Delta\mathbf{H}^{(p)} = \frac{1}{\tau'(\mathbf{H}^{(p)})}[\Delta\mathbf{u}^{(p)} + (\mathbf{u}^{(p)} - \tau(\mathbf{H}^{(p)}))]. \tag{2.41}$$

The incrementation (2.41) is relaxed by replacing the quantity $1/\tau'(\mathbf{H}^{(p)})$ by a constant quantity $\mu = 1/\max(\tau'(\mathbf{H}^{(p)}))$ in all the domain and during the whole iteration process as:

$$\Delta\mathbf{H}^{(p)} = \mu[\Delta\mathbf{u}^{(p)} + (\mathbf{u}^{(p)} - \tau(\mathbf{H}^{(p)}))]. \tag{2.42}$$

The linearization of $R_{n+1}(\mathbf{u}_{n+1})$ is given by

$$DR_{n+1}(\mathbf{u}_{n+1}) = \frac{\Delta \mathbf{H}_{n+1}^{(p)} - \Delta \mathbf{H}_n^{(p)}}{\Delta t} - A\Delta \mathbf{u}_{n+1}^{(p)}, \qquad (2.43)$$

which, after substitution of (2.41) yields the following relaxed linearized form

$$\underbrace{\tilde{D}R_{n+1}(\mathbf{u}_{n+1})}_{=\Psi}\Delta \mathbf{u}_{n+1}^{(p)} = \underbrace{-R_{n+1}(\mathbf{u}_{n+1}^{(p)}) - \frac{\mu}{\Delta t}(\mathbf{u}_{n+1}^{(p)} - \tau(\mathbf{H}_{n+1}^{(p)}))}_{=\Phi}, \qquad (2.44)$$

where

$$\Psi^{(p)} = \frac{\mu}{\Delta t} - A. \qquad (2.45)$$

The following iterative process is performed in order to obtain the solution to the nonlinear enthalpy equation at each time step:

1. From a converged solution at time $t = t_n$, initialize the temperature and enthalpy field: $p = 0$, $u_{n+1}^{(0)} = u_n$ and $H_{n+1}^{(0)} = H_n$.

2. Solve for a new temperature increment:

$$\Delta \mathbf{u}_{n+1}^{(p)} = \Psi^{(p)^{-1}}\Phi^{(p)}. \qquad (2.46)$$

3. Update the nodal temperature:

$$\mathbf{u}_{n+1}^{(p+1)} = \mathbf{u}_{n+1}^{(p)} + \Delta \mathbf{u}_{n+1}^{(p)}. \qquad (2.47)$$

4. Update the enthalpy according to the relaxed formula (2.42):

$$\mathbf{H}_{n+1}^{(p+1)} = \mathbf{H}_{n+1}^{(p)} + \mu[\mathbf{u}_{n+1}^{(p+1)} - \tau(\mathbf{H}_{n+1}^{(p)})] \qquad (2.48)$$

5. Set $p \leftarrow p + 1$ and go to step 2 unless until convergence is attained when $\|\Phi^{(p)}\| < tolerance$

The results that were acquired employing the pseudo-Newton relaxed linearization technique for the test problems from Sections 2.3 and 2.4 have been found to be (nearly) equal to those found using 'Voller's method' in combination with Elliott-Ockendon SOR. Thus, it can be concluded that the technique as proposed by Nedjar does not show any significant improvement with respect to reducing the 'stair-casing' effect.

Chapter 3

Conclusions

Based on the preceding chapters, the following conclusions can be drawn:

- When using an enthalpy scheme, it is advisable to apply the Kirchoff transformation, since it will result in faster convergence of the iterative scheme.

- The numerically obtained temperature, when plotted as function of the time, at a fixed location in space, shows 'stair-casing'. This appears to be inherent to the enthalpy approach.

- For the 'classical' Voller method, in combination with the Elliott-Ockendon SOR scheme, the 'stair-casing' effect is the most severe.

- The introduction of an 'superficial phase-change range', as proposed by Bhattacharya, can be used to reduce the stair-casing. The higher the Stefan number, the stronger the stair-casing is damped out.

- With respect to reducing the stair-casing effect, the method as proposed by Nedjar does not show much improvement, unfortunately.

- At this moment, it is difficult to say which of the discussed methods the best choice for solving the two-phase Stefan problem. Further research is therefor essential.

Bibliography

[1] V. Alexiades and A.D. Solomon. *Mathematical modeling of melting and freezing processes*. Hemisphere Publishing Corporation, 1993.

[2] M. Bhattacharya, T. Basak, and K.G. Ayappa. a fixed-grid finite element based enthalpy formulation for generalized phase change problems: Role of superficial mushy region. *Int. J. Heat and Mass Transf.*, 45:4881–4898, 2002.

[3] J.H. Brusche. Numerical modeling of optical phase-change recording. Internal report 04-04, Technische Universiteit Delft, 2004.

[4] C.K. Chun and S.O. Park. A fixed-grid finite-difference method for phase-change problems. *Num. Heat Transf., Part B*, 38:59–73, 2000.

[5] B. Nedjar. An enthalpy-based finite element method for nonlinear heat problems involving phase change. *Computers and Structures*, 80:9–21, 2002.